

Compound nucleus decay of ^{47}V : comparison between saddle point and scission point barriers in the $^{35}\text{Cl}+^{12}\text{C}$ and $^{23}\text{Na}+^{24}\text{Mg}$ reactions

T.J. Santos* and **B.V. Carlson**

Instituto Tecnológico de Aeronáutica, São José dos Campos, SP, Brazil

E-mail: nztiago@gmail.com, brettvc@gmail.com

One of the fundamental characteristics of nuclear multifragmentation process is the emission of complex fragments of intermediate mass. The statistical multifragmentation model provides a reasonably good description of the distribution of intermediate mass fragments. However, it does not furnish a complete physical description of the statistical decay, because it does not estimate the decay widths and lifetimes for emission. An extension of this model to include partial widths and lifetimes for emission interprets the fragmentation process as the near simultaneous limit of a series of sequential binary decays. In this formalism, the expression describing intermediate mass fragment emission is almost identical to that of light particle emission. Furthermore at lower temperatures, similar expressions have been shown to furnish a good description of very light intermediate mass fragment emission. But this is usually not considered a good approximation to the emission of heavier fragments. These emissions seem to be determined by the characteristics of the system at the saddle-point and its subsequent dynamical evolution rather than by the scission point. In this work we compare the barriers and decay widths of these different formulations of intermediate fragment emission and analyze the extent to which they remain distinguishable at high excitation energy in the $^{35}\text{Cl}+^{12}\text{C}$ and $^{23}\text{Na}+^{24}\text{Mg}$ reactions that populate the ^{47}V compound nucleus.

*X Latin American Symposium on Nuclear Physics and Applications (X LASNPA),
1-6 December 2013
Montevideo, Uruguay*

*Speaker.

1. Introduction

We know experimentally that an excited nuclear system can break up into several smaller nuclei, this is, complex fragments, protons and neutrons. This occurs when a large amount of energy (on the order of 2 or more MeV per nucleon) is deposited in it. This process of nuclear multifragmentation is observed in collisions between heavy ions at energies ranging from a few tens to a few hundreds of MeV per nucleon.

Theoretical and experimental studies of the phenomenon have received great attention from the nuclear physics community. Initially this was due to the fact that the fragment charge distribution follows a power law, which was interpreted as a sign of a phase transition in nuclear matter. However, several subsequent studies have shown that other mechanisms can also explain such behavior.

The study of the process of nuclear multifragmentation is not exhausted by the prospect of observing such a transition phase. Understanding how nuclear matter behaves when heated and compressed, as happens in the early stages of heavy-ion nuclear reactions leading to the nuclear multifragmentation process, is also of great importance in astrophysics for understanding the evolution of supernovae. Moreover, this phenomenon is of great theoretical interest in nuclear physics. A more complete study of this process would require the ability to describe the dynamical evolution of a quantum many-body system of strongly interacting constituents. An exact solution of this problem goes far beyond the limits of existing computational resources and formal theoretical tools. Therefore due to the complexity of the dynamics of such a many-body system and the richness of phenomena that it presents, many models and approaches have been used to describe its various facets.

The statistical approach to the problem assumes that the collision between two nuclei leads to a hot compound system in thermodynamical equilibrium. Differently from dynamical approaches, statistical models do not attempt to describe the evolution of the system from the initial stages of the collision.

2. Statistical emission model

One of the fundamental characteristics of nuclear multifragmentation is the emission of fragments of intermediate mass. The statistical multifragmentation model[1, 2, 3, 4] provides a reasonably good description of the distribution of intermediate mass fragments. However, it does not furnish a complete physical description of the statistical decay, because it does not estimate the decay widths and lifetimes for emission. In this model, the fragments are formed simultaneously during the final stage of the expansion of the hot nuclear system. When the multifragmentation statistical model is extended to include the calculation of partial widths, it can be interpreted as the nearly simultaneous decay limit of a sequential emission model. [5]

To obtain such a model, one first considers the multifragmentation of an initial nucleus Z_0, A_0 to be only approximately simultaneous. After organizing the fragments into the two fragments that are the first to separate one can then sum over all partitions that separate into the same first two fragments, Z_1, A_1 and Z_2, A_2 . The rate at which this happens is just the rate at which the two

fragments separate beyond their radius of nuclear interaction. This can be written as

$$-\frac{d}{dt}\omega_{tot}(\varepsilon_0, Z_0, A_0)_{\rightarrow Z_1 A_1, Z_2 A_2} = \frac{1}{(2\pi\hbar)^3} \int d^3 p d^3 r \frac{\hat{r} \cdot \vec{p}}{\mu} \theta(\hat{r} \cdot \vec{p}) \delta(r - R) \quad (2.1)$$

$$\times \int \omega_{tot}(\varepsilon_1, Z_1, A_1) \omega_{tot}(\varepsilon_2, Z_2, A_2) d\varepsilon_1 d\varepsilon_2 \delta\left(\varepsilon_0 - Q - V_B - \frac{p^2}{2\mu} - \sum_{j=1}^2 \varepsilon_j\right),$$

where $\omega_{tot}(\varepsilon, Z, A)$ is the total density of states of nucleus Z, A at excitation energy ε , Q is the Q-value of the reacton and V_B is the effective potential barrier. This expression can be simplified to

$$2\pi\Gamma_{Z_0 A_0 \rightarrow Z_1 A_1, Z_2 A_2} \omega_{tot}(\varepsilon_0, Z_0, A_0) = \int de \frac{2\mu e}{\pi\hbar^2} \sigma_{abs, Z_1 A_1 + Z_2 A_2}(e) \quad (2.2)$$

$$\times \int \omega_{tot}(\varepsilon_1, Z_1, A_1) \omega_{tot}(\varepsilon_2, Z_2, A_2) d\varepsilon_1 d\varepsilon_2 \delta(\varepsilon_0 - Q - e - \varepsilon_1 - \varepsilon_2),$$

The derivative on the left-hand side has been rewritten in terms of the partial decay width, $\Gamma_{Z_0 A_0 \rightarrow Z_1 A_1, Z_2 A_2}$ and the absorption cross section has been substituted for the geometrical cross section

$$\pi R^2 (1 - V_B/e) \rightarrow \sigma_{abs, Z_1 A_1 + Z_2 A_2}(e). \quad (2.3)$$

Here, intermediate mass fragment emission is described by an expression almost identical to the Weisskopf approximation to light particle emission. At lower temperatures, similar expressions have been shown to furnish a good description of very light intermediate mass fragment emission [6]. However, the emission of heavier fragments seems to be determined by the transition density at the saddle-point rather than at the scission point. [7, 8, 9] The saddle point model is essentially identical to the transition state model developed to describe the fission of heavier systems. However we do not expect a significant energy difference between the saddle and scission points in lighter systems. This suggests that the predictions of the saddle point model and an extended Hauser-Feshbach type scission should be similar in this case. Here we compare the barriers and decay widths of these different formulations of intermediate mass fragment emission.

For intermediate mass fragment emission the transition state model approximates the emission width in terms of the density of states at the saddle point barrier using a thermal excitation energy obtained by subtracting the collective rotational energy in the sticking limit. However it takes into account no additional effects of the angular momenta of the fragments nor of their relative motion. To estimate the emission width of the scission model of intermediate mass fragment emission, we extend the expression above to take into account all effects of (classical) angular momentum as well as energy conservation. We write

$$2\pi\Gamma(\varepsilon_0, \vec{J}_0; Z_1 A_1, Z_2 A_2) \rho_0(\varepsilon_0, \vec{J}_0) = \frac{1}{2(2\pi\hbar)^2} \int \delta(\hat{r} \cdot \vec{L}) d^3 L d\Omega de_r \quad (2.4)$$

$$\times \prod_{j=1}^2 \left(\rho_j(\varepsilon_j, \vec{J}_j) d\varepsilon_j d^3 J_j \right) \delta(\vec{J}_0 - \vec{L} - \vec{J}_1 - \vec{J}_2)$$

$$\times \delta\left(\varepsilon_0 - Q - e_r - \frac{L^2}{2\mu R_B^2} - V_B - \varepsilon_1 - \varepsilon_2\right).$$

To evaluate this expression, we use saddle point methods to evaluate most of the integrals, which also furnish the sticking limit of rotational motion at the scission point, and then use the high energy limit of the Fermi gas level density to write the remaining product of level densities in terms of the saddle and scission level densities that the GEMINI++ code expects.

Ericson and Strutinsky proposed such a statistical emission model taking into account classical angular momentum conservation. [13] The approximation to the partial width of this last equation is equivalent to the assumption of a classical transmission coefficient, for which transmission above the barrier is unity and below the barrier is null. This should be reasonable at high excitation energies. Furthermore, the expression taking into account quantum barrier transmission has been used previously to describe intermediate mass fragment emission from light nuclei. [14]

3. Results and discussion

We use the GEMINI++ code to perform the calculations. This code was written in C++ by R. J. Charity, [10] and is the successor to his FORTRAN code GEMINI. The GEMINI++ code calculates the decay of the compound nucleus as a series of binary sequential emissions of light or intermediate mass fragments or fission. The emission of intermediate mass fragments is in fact treated as asymmetric fission. The GEMINI++ code uses Monte Carlo sampling based on the partial decay widths of all processes. This has the advantage of allowing the inclusion of time differences between emissions, which permits the calculation of proximity effects between the fragments that can not be included in the conventional approach.

One of the basic differences between the saddle-point and scission-point calculations presented here are their barriers, which in both cases enter the density of states that determine the partial emission widths. As the deformation of a nucleus increases, it eventually reaches a form for which the surface tension can no longer counteract the Coulomb repulsion. This is the saddle point. For larger deformations, the nucleus will separate into two fragments, which occurs at the scission point. The saddle point possesses a special stability to deformations in certain directions, for which the energy passes through a minimum. The geometry of the saddle point, including the role of the fragment deformation, is fully determined by macroscopic energy calculations.

The deformations at the saddle and scission points are very similar for light nuclei. So, the deformation necessary for instability is almost the same as that needed to split the nucleus in two fragments. As the mass and charge of the nucleus increases the difference in deformation at the two points increases as well. This occurs due to the fact that the Coulomb repulsion is of long range, while the attractive surface tension is due to the short-range nuclear force. Thus the instability that leads to the fission of heavy nuclei occurs at a much smaller deformation than that at which the fragments actually separate. One would thus expect the saddle-point and scission-point barriers of light nuclei to be similar, while the saddle-point barrier of heavier nuclei should be much higher than the scission-point barrier.

The default mode of the code GEMINI++ uses the saddle point barriers of Sierk and Moretto's transition state density formalism [8] to predict the emission cross sections of complex fragments, which are appropriate for heavier systems. The transition-state model developed by Sanders et al. [9] is specifically adapted to the region of small mass and is quite successful in describing asymmetric fragmentation in this region. By using the saddle-point configuration as the transition

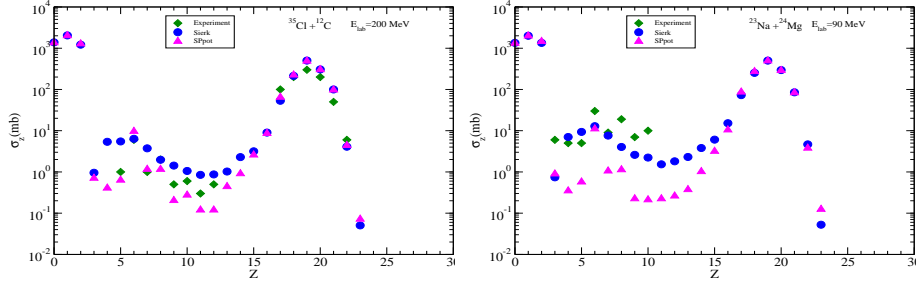


Figure 1: Cross sections of the $^{35}\text{Cl}+^{12}\text{C}$ and $^{23}\text{Na}+^{24}\text{Mg}$.

state, this model differs from the extended Hauser-Feshbach method, [7] which treats light-particle emission and heavy-fragment emission in a similar manner, with the fission probability taken as being proportional to the available phase space at the scission point.

In 1 we compare GEMINI++ calculations of intermediate mass fragment charge and mass yields with the experimental data of [7, 9] for the reactions $^{35}\text{Cl}+^{12}\text{C}$ and $^{23}\text{Na}+^{24}\text{Mg}$ at $E_{\text{lab}}=200$ and $E_{\text{lab}}=90$ MeV respectively. The two systems have different asymmetric masses, but both populate the ^{47}V compound nucleus. The calculations shown by the blue circles were performed with the default parameters of the code,[10] using Sierk saddle-point barriers [11] and Moretto's transition density formalism[8]. The saddle-point approximation to the fragment yields of Sanders et al. is given by the yellow points.[9] The pink triangles show the results from GEMINI++ with barriers obtained using the São Paulo potential at the scission radius. [12] The green diamonds represent the experimental data. The mass-asymmetric fission barriers are calculate following the procedure outlined by Sierk [11] in the case of the saddle-point calculations and using the São Paulo potential in the case of the scission-barrier calculations [12]. We observe that the calculations tend to underestimate the intermediate mass fragment yields at the lower excitation energy of 1.25 MeV per nucleon but are in better agreement at the higher energy of 1.79 MeV per nucleon. Both values of the excitation energy are well below the range of about 3-4 MeV per nucleon above which multifragmentation becomes important.

The calculations using the GEMINI++ code do not present good agreement with the experimental data in the intermediate mass region at low values of the center-of-mass energy but improve in agreement as the energy increases. Part of the discrepancy is due to that fact that the excitation spectrum of the fragments is represented by a continuum density of states. No discrete states are included in the calculations, but these states are extremely important at low energy, where little energy is available for exciting the fragments. In the calculations using the transition state density, the strong effect of the binding energy is taken into account by the adding a Wigner energy term to the the liquid drop energy. An alternative way to include this strong variation would be to incorporate shell effects in the level density.

In 2 and 3 we compare the Sierk saddle-point barriers (blue triangles) with the scission barriers of the São Paulo potential (red triangles) for the $^{35}\text{Cl} + ^{12}\text{C}$ and $^{23}\text{Na} + ^{24}\text{Mg}$ reaction, as a function of the charge and mass of the fragment of smaller charge. Although the results for both barriers follow very similar trends as a function of the mass, we find the scission barriers of the São Paulo

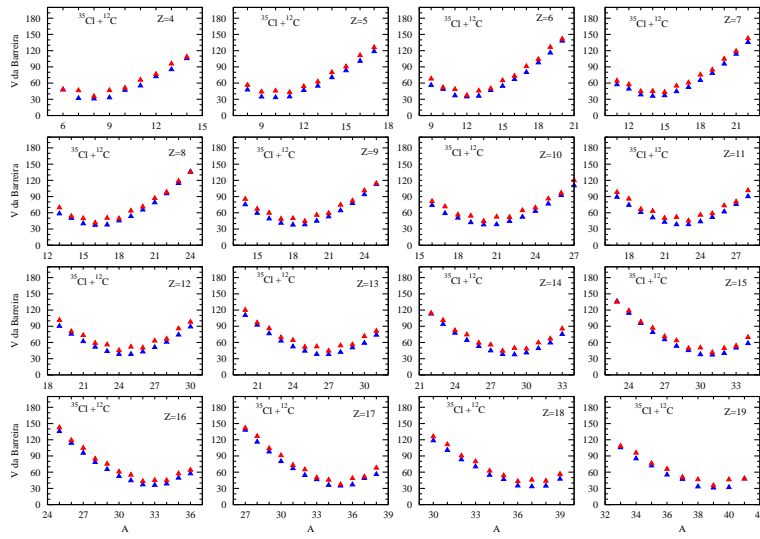


Figure 2: Comparison between the Sierk saddle-point barriers (blue triangles) and scission barriers of the São Paulo potential (red triangles) for the $^{35}\text{Cl} + ^{12}\text{C}$ reaction, as a function of the charge and mass of the fragment of smaller charge.

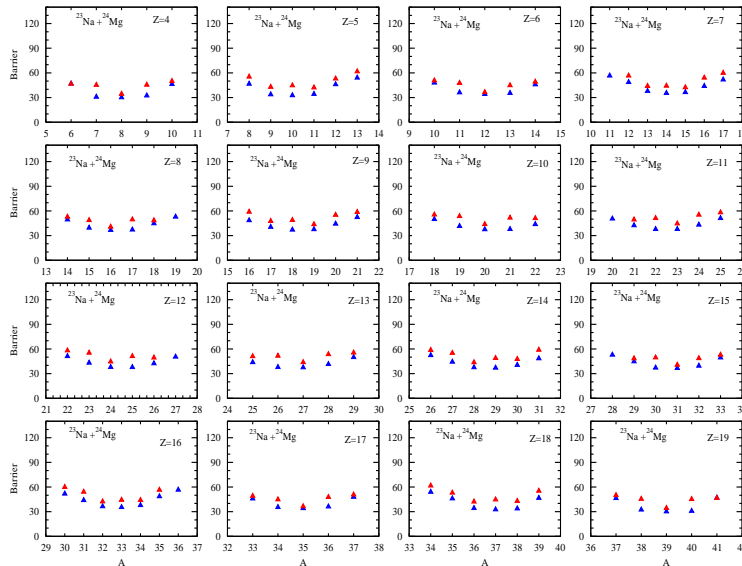


Figure 3: Comparison between the Sierk saddle-point barriers (blue triangles) and scission barriers of the São Paulo potential (red triangles) for the $^{23}\text{Na} + ^{24}\text{Mg}$ reaction, as a function of the charge and mass of the fragment of smaller charge.

potential to be large than the saddle point barriers, rather than smaller, as would be expected. This is in part due to the fact that fragment deformation is included in the definition of the saddle point geometry, which is based on a full calculations of the energy, while the fragments of the scission calculation are assumed to be spherical. However, irregularities in the differences between the two barriers suggest that the saddle-point barriers might still contain some contribution of the fragment energies.

In future work, we plan to extend the comparison of the barriers to heavier compound systems. Furthermore, we plan to extend our calculations of intermediate mass fragment emission to higher excitation energies and to heavier compound nuclear systems and to compare the results with those of the statistical multifragmentation model as well as with experimental data. We also plan to improve our implementation of the scission-point intermediate mass fragment emission model by including fragment deformation and the effects of nuclear expansion at high temperature in the determination of the scission point and intermediate mass fragment emission.

References

- [1] J. P. Bondorf, R. Donangelo, I. N. Mishustin, C. J. Pethick, H. Schulz and, K. Sneppen, *Statistical multifragmentation of nuclei I*, *Nucl Phys.* **A443**, 321 (1985).
- [2] J. Bondorf, R. Donangelo, I. N. Mishustin, H. Schulz, *Statistical multifragmentation of nuclei II*, *Nucl Phys.* **A444**, 460 (1985).
- [3] H. W. Barz, J. P. Bondorf, R. Donangelo, I. N. Mishustin, H. Schulz, *Statistical multifragmentation of nuclei III*, *Nucl.Phys.* **A448**, 753, (1986).
- [4] A. S. Botvina, A. S. Iljinov, I. N. Mishustin, J. P. Bondorf, R. Donangelo, K. Sneppen, *Statistical simulation of the break-up of highly excited nuclei*, *Nucl. Phys.* **A475**, 663 (1987).
- [5] B. V. Carlson, F. T. Dalmolin, M. Dutra, R. Donangelo, S. R. Souza, D. A. Toneli, *CERN Proceedings* 2012-002, 285 (2012).
- [6] T. J. Santos, B. V. Carlson, *AIP Conference Proceedings* 1529, 284 (2013).
- [7] T. Matsuse, C. Beck, R. Nouicer, D. Mahboub, *Extended Hauser-Feshbach method for statistical binary decay of light-mass system*, *Phys. Rev. C* **55**, 1380 (1997).
- [8] L. G. Moretto, *Statistical emission of large fragments: A general theoretical approach*, *Nucl. Phys.* **A247**, 211 (1975).
- [9] S. J. Sanders, *Fusion-fission in nuclear systems with $40 \leq A_{CN} \leq 80$* , *Phys. Rev. C* **44**, 2676 (1991).
- [10] R. J. Charity, in *Proceedings of the Joint ICTP-IAEA Advanced Workshop on Model Codes for Spallation Reactions* (IAEA, Trieste, Italy, 2008); edited by D. Filges, S. Leray, Y. Yariv, A. Mengoni, A. Stanculescu and G. Mank, INDC(NDS)-530, p. 139.
- [11] A. J. Sierk, *Mass-asymmetric fission of light nuclei*, *Phys. Rev. Lett.* **55**, 582 (1985).
- [12] L. C. Chamon, B. V. Carlson, L. R. Gasques, D. Pereira, C. D. Conti, M. A. G. Alvarez, M. S. Hussein, *Toward global description of the nucleus-nucleus interaction*, *Phys. Rev. C* **66**, 014610(2002).
- [13] T. Ericson and V. Strutinsky, *On angular distributions in compound nucleus processes*, *Nucl. Phys.* **8**, 284 (1958); **9**, 689 (1958).
- [14] B.V. Carlson, O. Civitarese, M. S. Hussein, A. Szanto de Toledo, *Multi-step compound model of heavy-ion fusion*, *Ann. Phys. (N.Y.)* **169**, 167 (1986).